

# Magnetic-Field-Induced Orientational Ordering of Alkaline Lyotropic Silicate–Surfactant Liquid Crystals

A. Firouzi,<sup>†</sup> D. J. Schaefer,<sup>†</sup> S. H. Tolbert,<sup>‡</sup> G. D. Stucky,<sup>‡</sup> and B. F. Chmelka<sup>\*†</sup>

Contribution from the Department of Chemical Engineering, Department of Chemistry, and Materials Department, University of California, Santa Barbara, California 93106

Received April 21, 1997<sup>⊗</sup>

**Abstract:** Macroscopically oriented silicate–surfactant liquid crystals are produced by slow cooling of lamellar and hexagonal mesophases through their isotropic–anisotropic phase transition in an 11.7 T magnetic field. Comparisons of *in situ* experimental and simulated <sup>2</sup>H NMR spectra quantify the degrees of orientational order in the silicate–surfactant liquid crystals. The overall orientations of the mesophases with respect to the applied magnetic field depend upon the combined diamagnetic susceptibilities of the individual molecular species in the multicomponent surfactant–silicate mixtures. As a result, macroscopic alignment of these liquid crystalline systems can be controlled by adjusting their composition: lamellar or hexagonal domains are shown to adopt different orientations, according to the diamagnetic susceptibilities of different organic additives present in otherwise identical mixtures. These results demonstrate the utility of liquid crystal processing strategies for organizing inorganic–organic hybrid materials over mesoscopic and macroscopic length scales.

## Introduction

The discovery<sup>1</sup> that mixtures of network-forming inorganic species and surfactants self-assemble into mesostructured materials has broadened considerably synthetic strategies and application opportunities in the field of inorganic–organic composite solids, particularly those with mesoscopic order.<sup>1–13</sup> Such materials can often be produced with rigid inorganic frameworks that result from dense cross-linking of the inorganic

species (most commonly metal oxides), and can be formed in a variety of mesoscopically ordered structures that are closely related to those observed in well-studied lyotropic liquid crystal<sup>14</sup> and block copolymer<sup>15</sup> systems. Materials with periodicities ranging from 25 Å to well over 100 Å have been made by using surfactant structure-directing agents for a wide variety of mixture compositions and conditions.<sup>1–13</sup> Moreover, this periodicity can often be exploited by calcining (i.e., heating under an oxidizing atmosphere) the mesophase to decompose the surfactant species to produce high surface-area, high void-volume, and mesoscopically ordered porous inorganic materials. Much insight into the cooperative self-assembly process governing formation of inorganic–organic mesophase materials has been gained by using conditions where thermodynamic equilibrium is established in the absence of polymerization of the inorganic species.<sup>5</sup> In particular, anionic silicate species under highly alkaline conditions (pH ≥ 12) and at moderate temperatures (≤ 100 °C) remain unpolymerized in aqueous solutions, and under such conditions it is possible to produce silicate–surfactant mesophases with true liquid crystalline properties.<sup>5–7</sup>

In this paper, we exploit for the first time liquid crystalline processing strategies to align macroscopically and characterize quantitatively unpolymerized silicate–surfactant mesophases, which can be used as intermediates for the preparation of oriented composite or mesoporous solids. When liquid crystalline properties are present, orientational ordering in magnetic,<sup>16</sup> electric,<sup>17</sup> or shear fields<sup>18</sup> can be used to generate macroscopic

<sup>†</sup> Department of Chemical Engineering.

<sup>‡</sup> Department of Chemistry and Materials Department.

<sup>⊗</sup> Abstract published in *Advance ACS Abstracts*, September 1, 1997.

(1) (a) Kresge, C. T.; Leonowicz, M. E.; Roth, W. J.; Vartuli, J. C.; Beck, J. S. *Nature* **1992**, *359*, 710–712. (b) Beck, J. S.; Vartuli, J. C.; Roth, W. J.; Leonowicz, M. E.; Kresge, C. T.; Schmitt, K. D.; Chu, C. T.-W.; Olson, D. H.; Sheppard, E. W.; McCullen, S. B.; Higgins, J. B.; Schlenker, J. L. *J. Am. Chem. Soc.* **1992**, *114*, 10834–10843. (c) Beck, J. S.; Vartuli, J. C.; Kennedy, G. J.; Kresge, C. T.; Roth, W. J.; Schramm, S. E. *Chem. Mater.* **1994**, *6*, 1816–1821.

(2) Monnier, A.; Schüth, F.; Huo, Q.; Kumar, D.; Margolese, D. I.; Maxwell, R. S.; Stucky, G. D.; Krishnamurty, M.; Petroff, P.; Firouzi, A.; Janicke, M.; Chmelka, B. F. *Science* **1993**, *261*, 1299–1303.

(3) (a) Huo, Q.; Margolese, D. I.; Ciesla, U.; Demuth, D. G.; Feng, P.; Gier, T. E.; Sieger, P.; Firouzi, A.; Chmelka, B. F.; Schüth, F.; Stucky, G. D. *Chem. Mater.* **1994**, *6*, 1176–1191. (b) Huo, Q.; Margolese, D. I.; Ciesla, U.; Feng, P.; Gier, T. E.; Sieger, P.; Leon, R.; Petroff, P. M.; Schüth, F.; Stucky, G. D. *Nature* **1994**, *368*, 317–321.

(4) (a) Huo, Q.; Leon, R.; Petroff, P. M.; Stucky, G. D. *Science* **1995**, *268*, 1324–1327. (b) Huo, Q.; Margolese, D. I.; Stucky, G. D. *Chem. Mater.* **1996**, *8*, 1147–1160.

(5) Firouzi, A.; Atef, F.; Oertli, A. G.; Stucky, G. D.; Chmelka, B. F. *J. Am. Chem. Soc.* **1997**, *119*, 3596–3610.

(6) Firouzi, A.; Kumar, D.; Bull, L. M.; Besier, T.; Sieger, P.; Huo, Q.; Walker, S. A.; Zasadzinski, J. A.; Glinka, C.; Nicol, J.; Margolese, D. I.; Stucky, G. D.; Chmelka, B. F. *Science* **1995**, *267*, 1138–1143.

(7) Firouzi, A.; Stucky, G. D.; Chmelka, B. F. *Synthesis of Microporous Materials*; Ocelli, M. L., Kessler, H., Eds.; Marcel Dekker, Inc.: New York, 1996; pp 379–389.

(8) (a) Chen, C. Y.; Li, H. X.; Davis, M. E. *Microporous Mater.* **1993**, *2*, 17–26. (b) Chen, C. Y.; Burkett, S. L.; Li, H. X.; Davis, M. E. *Microporous Mater.* **1993**, *2*, 27–34. (c) Chen, C. Y.; Xiao, S. Q.; Davis, M. E. *Microporous Mater.* **1995**, *4*, 1–20.

(9) (a) Tanev, P. T.; Pinnavaia, T. J. *Science* **1995**, *267*, 865–867. (b) Tuel, A.; Gontier, S. *Chem. Mater.* **1996**, *8*, 114–122. (c) Attard, G. S.; Glyde, J. C.; Göltner, C. G. *Nature* **1995**, *378*, 366–368. (d) Fyfe, C. A.; Fu, G. J. *J. Am. Chem. Soc.* **1995**, *117*, 9709–9714.

(10) (a) Cheng, C.; Luan, Z.; Klinowski, J. *Langmuir* **1995**, *11*, 2815–2819. (b) Steel, A.; Carr, S. W.; Anderson, M. W. *Chem. Mater.* **1995**, *7*, 1829–1832. (c) Steel, A.; Carr, S. W.; Anderson, M. W. *J. Chem. Soc., Chem. Commun.* **1994**, 1571–1572.

(11) (a) Yang, H.; Kuperman, A.; Coombs, N.; Mamiche-Afara, S.; Ozin, G. A. *Nature* **1996**, *379*, 703–705. (b) Raman, N. K.; Anderson, M. T.; Brinker, C. J. *Chem. Mater.* **1996**, *8*, 1682–1701.

(12) (a) Aksay, I. A.; Trau, M.; Manne, S.; Honma, I.; Yao, N.; Zhou, L.; Fenter, P.; Eisenberger, P. M.; Gruner, S. M. *Science* **1996**, *273*, 892–898. (b) Braun, P. V.; Osenar, P.; Stupp, S. I. *Nature* **1996**, *380*, 325–328. (c) Yang, H.; Coombs, N.; Ozin, G. A. *Nature* **1997**, *386*, 692–695.

(13) (a) Liu, J.; Kim, A. Y.; Virden, J. W.; Bunker, B. C. *Langmuir* **1995**, *11*, 689–692. (b) Wang, L.; Liu, J.; Exarhos, G. J.; Bunker, B. C. *Langmuir* **1996**, *12*, 2663–2669.

(14) (a) Tiddy, G. J. T. *Phys. Rep.* **1980**, *57*, 1–46. (b) Charvolin, J.; Tardieu, A. *Solid State Phys.* **1978**, *14*, 209–257.

(15) (a) Bates, F. S.; Fredrickson, G. H. *Annu. Rev. Phys. Chem.* **1990**, *41*, 522–557. (b) Bates, F. S.; Schulz, M. F.; Khandpur, A. K.; Förster, S.; Rosedale, J. H. *Faraday Discuss.* **1994**, *98*, 7–18. (c) Fredrickson, G. H.; Helfand, E. *J. Chem. Phys.* **1987**, *87*, 697–705. (d) Winey, K. I.; Thomas, E. L.; Fetter, L. J. *J. Chem. Phys.* **1991**, *95*, 9367–9375.

sample anisotropy. While such alignment often exists over length scales that are much larger than a material's molecular and mesoscopic structures, these shorter length scales are nevertheless important to establishing macroscopic orienting behavior. In particular, the rich compositional behavior of multicomponent silicate–surfactant liquid crystals can be tuned to allow appreciable control over the phase(s) achieved, as well as the directions the mesophase morphologies orient with respect to the aligning field. Consequently, it is necessary to characterize these materials over a wide range of structural dimensions (often spanning  $10^{-9}$ – $10^{-2}$  m), to establish the key parameters and conditions central to their orientational ordering properties.

While techniques such as small-angle X-ray diffraction (XRD) and polarized optical microscopy (POM) can provide information about liquid crystal structure and alignment, deuterium ( $^2\text{H}$ ) nuclear magnetic resonance (NMR) spectroscopy is a convenient means for quantitatively correlating the effects of different molecular variables on mesophase morphologies and their alignment. The  $^2\text{H}$  NMR line shape is sensitive to motional averaging of the electric field gradient tensors of individual C– $^2\text{H}$  bonds, and thus can be used to examine local and mesoscopic environments of deuterated species.<sup>19</sup> For example, in liquid crystalline systems containing deuterated surfactant molecules, rapid molecular mobility results in anisotropic averaging of the  $^2\text{H}$  electric field gradient tensors within individual aggregates, which for an unoriented sample leads to a scaled powder  $^2\text{H}$  NMR spectrum that reflects aggregate geometry and mesophase morphology.<sup>20,21</sup> Furthermore, the directional dependence of the quadrupolar interaction allows the distribution of aggregate orientations to be measured over macroscopic sample length scales. This is useful for aligned materials, which possess anisotropic distributions of domain orientations that concentrate intensity in certain regions of the  $^2\text{H}$  NMR spectrum, and which can be quantified with the aid of spectral simulations or directly using the DECODER NMR technique.<sup>19</sup>

Deuterium NMR spectroscopy can be used both to characterize aggregate structure and to quantify the degree of alignment in deuterated silicate–surfactant liquid crystalline mesophases. Here, orientational ordering is induced by processing samples within an 11.7-T magnetic field, which provides the opportunity to monitor simultaneously changes in local liquid crystalline structure and macroscopic domain alignment *in situ* with temperature. Such combined information yields insight into the energetics of the alignment process, including kinetic barriers and aggregate effects.

## Experimental Section

Mesophase morphology and orientational ordering of lamellar and hexagonal silicate–surfactant liquid crystals were examined experimentally by using  $^2\text{H}$  NMR spectroscopy of  $\alpha$ -deuterated cetyltrimethylammonium surfactant species [ $\text{H}_3\text{C}-(\text{CH}_2)_{14}-\text{CD}_2-\text{N}(\text{CH}_3)_3^+$ ]. Aggregate geometry (e.g., sheets or cylinders), mean local order parameters, aggregate and domain diamagnetic susceptibilities, and aggregate orientation distributions were established by using  $^2\text{H}$  NMR methods that have been widely used to study such features in conventional lyotropic liquid crystals.<sup>20,21</sup> The procedure for deuterating the cationic surfactant cetyltrimethylammonium bromide (CTAB) at the  $\alpha$ -carbon position has been outlined elsewhere.<sup>5</sup> The syntheses of silicate–surfactant liquid crystal mesophases and details of the  $^2\text{H}$  NMR measurements and simulations are discussed below.

### Preparation of Silicate–Surfactant Liquid Crystals at High pH.

Aqueous isotropic surfactant precursor solutions were prepared containing 5–12 wt % of  $\alpha$ -deuterated CTAB and in some cases varying amounts of organic solute (e.g., benzene or hexanol); solutions were mixed and gently heated (40–50 °C) to dissolve the surfactant. An aqueous silicate precursor solution (prepared as outlined previously<sup>5</sup>) contained an overall molar composition of 1.0SiO<sub>2</sub>:1.1tetramethylammonium hydroxide (TMAOH):42H<sub>2</sub>O:14.1CH<sub>3</sub>OH, and has been shown to yield a pH 12.5 mixture containing predominantly double–four–ring (D4R) silicate oligomers.<sup>5</sup> The presence of CH<sub>3</sub>OH appears to be important for achieving a high degree of macroscopic mesophase alignment in magnetic fields under these conditions.<sup>22,23</sup> In a typical preparation, the dilute silicate precursor solution was added at room temperature to the dilute aqueous isotropic surfactant solution and stirred for 30 min to several days to allow equilibration. Hexagonal silicate–surfactant liquid crystals were prepared by using little or no organic additives; benzene:CTAB molar ratios that are less than 2.3 yield a hexagonal morphology at room temperature. Lamellar phases were produced by using larger quantities of benzene (molar ratios of benzene:CTAB greater than 3.5) or by the addition of straight chain alcohols such as hexanol (hexanol:CTAB molar ratios of 1.3 were used) to swell the hydrophobic regions of the aggregates, leading to reduced curvature of the hydrophobic–hydrophilic aggregate interfaces.<sup>24,25</sup> All liquid crystal phases were identified by  $^2\text{H}$  NMR quadrupolar splittings, in combination with separate small-angle X-ray scattering measurements.<sup>5</sup>

**Mesophase Alignment in a Strong Magnetic Field.** Orientational ordering of the lamellar and hexagonal silicate–surfactant liquid crystals was achieved in a 11.7 T magnetic field by heating the samples above their respective anisotropic–isotropic phase transitions (50 to 90 °C, depending on sample composition) such that the respective  $^2\text{H}$  NMR spectra each displayed a single isotropic peak. Previous examination of the phase behavior of silicate–surfactant liquid crystals has shown good agreement between the anisotropic–isotropic transition observed in  $^2\text{H}$  NMR and the loss of long-range order as determined by small-angle X-ray scattering.<sup>5</sup> Isotropic samples were subsequently cooled gradually (5 °C increments/h) to ambient temperature while in the high magnetic field. Thermal cycling near the anisotropic–isotropic transition temperature was in some instances used to improve the alignment of the liquid crystal phase.<sup>22,23</sup> During the cooling process, *in situ*  $^2\text{H}$  NMR measurements were conducted to probe the degree of orientational ordering.

**$^2\text{H}$  NMR Spectroscopy.** Deuterium NMR measurements were performed at 11.7 T on a Chemagnetics CMX-500 spectrometer, using a standard quadrupolar–echo pulse sequence with  $\pi/2$  pulse lengths of 4–6  $\mu\text{s}$ , a 50- $\mu\text{s}$  echo delay, a recycle delay of 0.25 s, and 3600–7200 signal accumulations. The samples were placed in specially designed 10-mm Kel-F containers with threaded caps to prevent any

(16) (a) Schnepf, W.; Disch, S.; Schmidt, C. *Liq. Cryst.* **1993**, *14*, 843–852. (b) Gutman, H.; Loewenstein, A.; Luz, Z.; Poupko, R.; Zimmermann, H. *Liq. Cryst.* **1991**, *9*, 607–616. (c) Gutman, H.; Luz, Z.; Wachtel, E. J.; Poupko, R.; Charvolin, J. *Liq. Cryst.* **1990**, *7*, 335–351. (d) Jansson, M.; Thurmond, R. L.; Trouard, T. P.; Brown, M. F. *Chem. Phys. Lipids* **1990**, *54*, 157–170.

(17) (a) Amundson, K.; Helfand, E.; Quan, X.; Hudson, S. D.; Smith, S. D. *Macromolecules* **1994**, *27*, 6559–6570. (b) Winsor, P. A. In *Liquid Crystals and Plastic Crystals*; Gray, G. W., Winsor, P. A., Eds.; Ellis Harwood Ltd.: Chichester U.K., 1974; Vol 2, p 122.

(18) (a) Lukaschek, M.; Grabowski, D. A.; Schmidt, C. *Langmuir* **1995**, *11*, 3590–3594. (b) Powers, L.; Pershan, P. S. *Biophys. J.* **1977**, *20*, 137–152. (c) Powers, L.; Clark, N. A. *Proc. Natl. Acad. Sci. U.S.A.* **1977**, *72*, 840–843. (d) Müller, J. A.; Stein, R. S.; Winter, H. H. *Rheol. Acta* **1996**, *35*, 160–167. (e) Barclay, G. G.; McNamee, S. G.; Ober, C. K.; Papathomas, K. I.; Wang, D. W. *J. Polym. Sci. Part A: Polym. Chem.* **1992**, *30*, 1845–1853.

(19) (a) Schmidt-Rohr, K.; Spiess, H. W. *Multidimensional Solid-State NMR and Polymers*; Academic Press: San Diego, 1994. (b) Spiess, H. W. *Colloid Polym. Sci.* **1983**, *261*, 193–209.

(20) Seelig, J. *Q. Rev. Biophys.* **1977**, *10*, 353–418.

(21) (a) Blackburn, J. C.; Kilpatrick, P. K. *Langmuir* **1992**, *8*, 1679–1687. (b) Halle, B.; Wennerström, H. *J. Chem. Phys.* **1981**, *75*, 1928–1943.

(22) Firouzi, A. Ph.D. Dissertation, University of California, Santa Barbara, 1997.

(23) Firouzi, A.; Atef, F.; Stucky, G. D.; Chmelka, B. F., manuscript in preparation.

(24) Israelachvili, J. N. *Intermolecular & Surface Forces*; Academic Press: London, 1991.

(25) A dimensionless parameter  $g = V/a_0l_c$  can be used to predict the preferred configuration of the surfactant assembly, where  $V$  is the effective volume of the hydrophobic chain,  $a_0$  is the effective aggregate surface area available per hydrophilic head group, and  $l_c$  is the critical hydrophobic chain length.<sup>23</sup>

loss of solvent or organic solute during heating. In measuring the  $^2\text{H}$  NMR line shapes and accompanying quadrupolar splittings, as a function of temperature, the samples were allowed to equilibrate for 30 min at each temperature. Longer waiting periods resulted in no discernible changes in the  $^2\text{H}$  NMR spectra acquired. The experimental  $^2\text{H}$  NMR spectra, in conjunction with  $^2\text{H}$  NMR simulations (discussed below), allow quantitative determination of aggregate orientation distributions, establish the signs of the aggregate and domain diamagnetic susceptibilities, and permit the local order parameters to be determined for lamellar and hexagonal silicate–surfactant liquid crystal phases. Deuterium NMR measurements were also performed on each of the aligned materials at room temperature, following macroscopic reorientation of the samples through an angle of  $90^\circ$  with respect to the applied field. Comparison of the resulting  $^2\text{H}$  NMR spectra with spectra simulated by using the same parameters determined prior to the rotation, modified only to account for the  $90^\circ$  rotation imposed, allows the distribution of domain directors to be established unambiguously.

### Theory

**$^2\text{H}$  NMR of Lyotropic Liquid Crystals.** The  $^2\text{H}$  NMR line shape is governed by the coupling between the electric quadrupole moment ( $eQ$ ) of a given quadrupolar  $^2\text{H}$  nucleus (spin  $I=1$ ) with its local electric field gradient (EFG). Due to the orientation dependence of the NMR frequency, molecular dynamics can have dramatic effects on the measured spectra. In a liquid crystalline phase, rapid anisotropic molecular motions occur within the anisotropic geometries of the individual aggregates to produce a time-averaged quadrupolar interaction.<sup>20</sup> The corresponding residual quadrupolar splitting and the  $^2\text{H}$  NMR line shape contain information on the mean shape and asymmetry of the aggregate, the average local order parameter of the  $\text{C}-^2\text{H}$  bonds, and the overall distribution of the aggregate director axes.

Following Seelig,<sup>20</sup> the quadrupolar splitting  $\Delta\nu_{\text{single domain}}^{\text{LC}}$  (i.e., the doublet) of a single domain of an uniaxial lyotropic liquid crystal (LLC) phase (e.g., a lamellar or hexagonal phase, which are comprised of a collection of axially symmetric flat sheets or cylindrical aggregates, respectively) can be written as:

$$\Delta\nu_{\text{single domain}}^{\text{LC}} = |2\bar{\delta} \cdot \frac{1}{2}(3 \cos^2 \theta_{\text{DL}} - 1)| \quad (1A)$$

where

$$\bar{\delta} = \delta \cdot \frac{1}{2}(3 \cos^2 \theta_{\text{PM}} - 1)_{\text{M}} \cdot \frac{1}{2}(3 \cos^2 \theta_{\text{MD}} - 1)_{\text{D}} \quad (1B)$$

and  $\delta$  and  $\bar{\delta}$  are static and time-averaged anisotropy parameters, respectively, LC denotes a liquid crystal, and the terms in broken brackets  $\langle \rangle$  represent values that are time averaged during the  $10^{-5}$ – $10^{-4}$  s time scale of the  $^2\text{H}$  NMR experiment. Referring to Figure 1a,  $\theta_{\text{PM}}$  is defined as the angle between the orientation of a given  $\text{C}-^2\text{H}$  bond ( $P$ ), which coincides with the unique axis of the principal axes system of the  $^2\text{H}$  EFG tensor, and the orientation of the surfactant molecular axis ( $M \equiv M_s$ ). The term  $\frac{1}{2}(3 \cos^2 \theta_{\text{PM}} - 1)_{\text{M}}$  is often referred to as the local order parameter ( $S_{\text{CD}}$ ) of the  $\text{C}-^2\text{H}$  bonds<sup>20</sup> and generally increases with decreasing temperature, indicating that local ordering increases as molecular mobility is reduced.<sup>21</sup>

The term  $\frac{1}{2}(3 \cos^2 \theta_{\text{MD}} - 1)_{\text{D}}$  represents the average molecular-axis orientation that results from rapid translational diffusion of a surfactant molecule within a given aggregate and depends on the angle  $\theta_{\text{MD}}$  between the surfactant molecular axis ( $M_s$ ) and the director optical axis of the aggregate ( $D$ ), the latter being normal to the bilayer planes of a lamellar phase (Figure 1a) or parallel to the cylindrical axes of aggregates in a

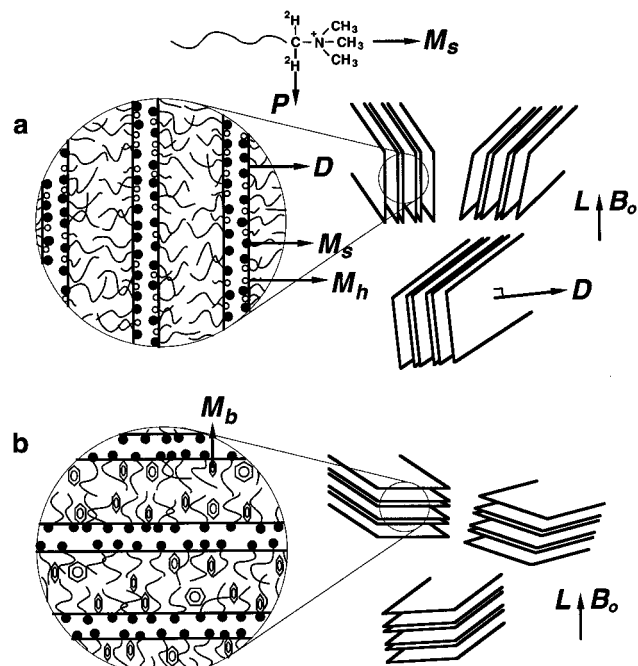


**Figure 1.** Schematic representations of lamellar silicate–surfactant liquid crystal domains that have been aligned in a magnetic field. Part a depicts a lamellar phase synthesized by using cationic cetyltrimethylammonium surfactant species ( $\text{CTA}^+$ ), hexanol, and anionic double–four–ring (D4R) silicate oligomers in an alkaline aqueous solution. The molecular director axes of the  $\text{CTA}^+$  surfactant and hexanol molecules ( $M_s$  and  $M_h$ , respectively) point along the long axes of these molecules and are parallel to the domain director of the planar aggregates ( $D$ ) (i.e.,  $M_s \parallel M_h \parallel D$ ). The principal axes system ( $P$ ) is defined by the direction of the  $\alpha\text{-C}-^2\text{H}$  bond. Due to the negative molecular diamagnetic susceptibilities of both  $\text{CTA}^+$  and hexanol, the overall domain susceptibility is negative ( $\Delta\chi^d < 0$ , eq 4) and the domains are observed (Figure 3b) to orient with their directors on average perpendicular to the applied magnetic field ( $B_0$  or  $L$ , laboratory frame) (i.e.,  $\langle D \rangle \perp L$ ). Part b depicts a lamellar phase synthesized by using  $\text{CTA}^+$ , benzene, and D4R silicate species. The molecular director of the benzene molecule ( $M_b$ ) is defined to lie in the plane of the benzene ring, which orients parallel to  $M_s$  for steric reasons. Thus, the molecular directors of the organic components of the composite again lie parallel to the domain director (i.e.,  $M_s \parallel M_b \parallel D$ ). Because of the large positive diamagnetic susceptibility of benzene, however, the overall domain susceptibility is positive ( $\Delta\chi^d > 0$ ) and the lamellar domains orient with their directors on average parallel to the applied field (i.e.,  $\langle D \rangle \parallel L$ , Figure 4b).

hexagonal phase (Figure 2a). The very fast local motions of the aliphatic surfactant chains, with effective correlation times  $\tau_c^{\text{M}} \approx 10^{-11}$ – $10^{-10}$  s, and fast translational diffusion of the surfactant molecules within the aggregates, with effective correlation times  $\tau_c^{\text{D}} \approx 10^{-9}$ – $10^{-7}$  s, create a time-averaged electric field gradient with its unique axis (the  $z$ -direction) parallel to the aggregate optical axis  $D$ .<sup>21</sup>

Finally, the term  $\frac{1}{2}(3 \cos^2 \theta_{\text{DL}} - 1)$  depends on the orientation  $\theta_{\text{DL}}$  of an individual liquid crystal domain, each of which is a collection of self-assembled aggregates with a common director orientation  $D$  with respect to the direction of the applied magnetic field  $B_0$ , which establishes the  $z$ -axis of the laboratory frame of reference  $L$  (Figures 1a and 2a). Typically, a domain of aggregates in a viscous liquid crystal phase is, to a good approximation, immobile on the time scale of the NMR measurement, so that mesophase domain orientations can be considered time independent.<sup>21</sup>

For an isotropic distribution of liquid crystalline domains, eq 1 may be integrated over all possible angles  $\theta_{\text{DL}}$  to obtain a scaled powder NMR spectrum. In this case, the  $^2\text{H}$  quadrupolar

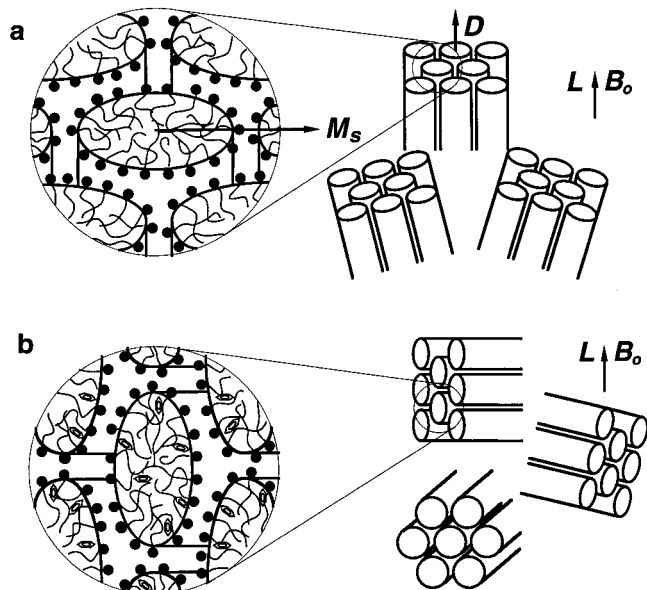


**Figure 2.** Schematic representations of hexagonal silicate–surfactant liquid crystal domains that have been aligned in a magnetic field. Part a depicts a hexagonal phase synthesized by using cationic CTA<sup>+</sup> and anionic D4R silicate species in an alkaline aqueous solution. As in Figure 1a, the molecular director of the CTA<sup>+</sup> surfactant ( $M_s$ ) points along the long axis of the molecule, and unlike the lamellar case,  $M_s$  is perpendicular to the domain director of the cylindrical aggregates ( $D$ ) (i.e.,  $M_s \perp D$ ). The negative molecular diamagnetic susceptibility of the CTA<sup>+</sup> molecules combined with the orthogonal relationship between the molecular and domain directors produce an overall positive domain susceptibility ( $\Delta\chi^d > 0$ , eq 4). As a result, these hexagonal domains orient with their optical directors on average parallel to the applied magnetic field ( $\mathbf{B}_0$  or  $L$ , laboratory frame) (i.e.,  $\langle D \rangle \parallel L$ , Figure 5b). Part b shows a hexagonal phase synthesized by using CTA<sup>+</sup>, benzene, and D4R silicate species. The molecular director of the benzene molecule ( $M_b$ ) is defined to lie in the plane of the ring and adopts, for steric reasons, a preferred orientation parallel to  $M_s$ . Thus, the molecular directors of the organic components of the composite are perpendicular to the domain director (i.e.,  $M_s \parallel M_b \perp D$ ). Due to the large positive diamagnetic susceptibility of the benzene molecules and the orthogonal relationship between molecular and domain directors, the overall domain susceptibility is negative ( $\Delta\chi^d < 0$ ), so that the hexagonal domains orient with their directors on average perpendicular to the applied field (i.e.,  $\langle D \rangle \perp L$ , Figure 6b).

splitting  $\Delta\nu_{\text{powder}}^{\text{LC}}$  between the two singularities is given by:

$$\Delta\nu_{\text{powder}}^{\text{LC}} = |\delta \cdot S_{\text{CD}} \cdot \frac{1}{2} \langle 3 \cos^2 \theta_{\text{MD}} - 1 \rangle_{\text{D}}| \quad (2)$$

As shown in Figure 1a, for bilayer planes in a lamellar ( $L_\alpha$ ) mesophase, the surfactant molecular axes  $M_s$  are on average parallel to their respective aggregate director axis  $D$ , so that  $\theta_{\text{MD}}$  is on average  $0^\circ$ . This is in contrast to the situation shown in Figure 2a for cylinders in a hexagonal ( $H_\alpha$ ) mesophase, where  $M_s$  is on average perpendicular to  $D$ , so that on average  $\theta_{\text{MD}}$  is  $90^\circ$ . Thus,

$$\Delta\nu_{\text{powder}}^{L\alpha} = \delta \cdot S_{\text{CD}} \cdot (1) \quad (3A)$$

and

$$\Delta\nu_{\text{powder}}^{H\alpha} = \delta \cdot S_{\text{CD}} \cdot \left(\frac{1}{2}\right) \quad (3B)$$

which shows that for equal order parameters ( $S_{\text{CD}}$ ), a lamellar LLC phase is expected to yield a quadrupolar splitting that is twice as large as that for a hexagonal LLC morphology. For

micellar solutions or solutions containing amphiphilic molecules that are below their critical micelle concentration (CMC), the surfactant molecules experience rapid and isotropic motions. This results in the overall anisotropic term  $\langle 3 \cos^2 \theta_{\text{PL}} - 1 \rangle_L$  being effectively averaged to zero on the time scale of the NMR measurement, where  $\theta_{\text{PL}}$  is the angle between an individual C–<sup>2</sup>H bond ( $P$ ) and the laboratory frame of reference  $L$ . The <sup>2</sup>H NMR spectra of isotropic micellar phases and surfactant solutions below their CMC, such as those containing low concentrations of the  $\alpha$ -deuterated cetyltrimethylammonium surfactant species (CTA<sup>+</sup>) considered here, thus consist of narrow isotropic <sup>2</sup>H peaks.<sup>5–7</sup>

#### Macroscopic Alignment of Lyotropic Liquid Crystals.

Generally, the self-assembly of a lyotropic liquid crystal in the absence of an orienting field leads to a random distribution of domain orientations. However, when a lyotropic liquid crystal phase is subjected to a suitably strong external field, such as magnetic<sup>16</sup> or electric<sup>17</sup> fields or a shear flow,<sup>18</sup> the initially randomly oriented domains and corresponding aggregate directors  $D$  can be oriented over sample-size length scales. For example, a strong magnetic field induces alignment of a liquid crystal because of the interaction between the field and the anisotropy of the diamagnetic susceptibilities  $\Delta\chi^m = \chi_{\parallel}^m - \chi_{\perp}^m$  of the constituent molecules, where  $\chi_{\parallel}^m$  and  $\chi_{\perp}^m$  are the parallel and perpendicular diamagnetic susceptibility components of a given molecule  $m$ . This applies to all of the constituent molecules found in the aggregates comprising an arbitrary liquid crystal domain, including the surfactant species, the inorganic counterions, organic solutes, and cosolvent species.

Although the magnetic interaction energy associated with  $\Delta\chi^m$  of an individual molecule is small ( $\approx 10^{-6}kT$  in a 10 T field at room temperature), the additive effects contributed by all molecules in a given domain of self-assembled aggregates can collectively overcome the thermal disordering produced by Brownian aggregate motions and thereby allow orientational ordering to occur.<sup>26</sup> Alignment of an uniaxial liquid crystal domain in a magnetic field thus results from the interaction of the applied field with the collective diamagnetic susceptibility  $\Delta\chi^d$  of the domain given by:

$$\Delta\chi^d = \chi_{\parallel}^d - \chi_{\perp}^d = \sum_i N_i \Delta\chi_i^m \cdot \frac{1}{2} \langle 3 \cos^2 \theta_{\text{MD}} - 1 \rangle_{\text{D}} \quad (4)$$

where  $\chi_{\parallel}^d$  and  $\chi_{\perp}^d$  are the diamagnetic susceptibility components of a given domain ( $d$ ) that are parallel and perpendicular, respectively, to its director axis  $D$ ,  $N_i$  is the total number of molecules of type  $i$ , and the summation is over all types of molecules in the domain. The orientation-dependent contribution to the free energy  $G^{\text{align}}$  of a single domain of aggregates depends both on  $\Delta\chi^d$  (which includes  $\theta_{\text{MD}}$ ) and on the angle  $\theta_{\text{DL}}$  between the director axis  $D$  of the self-assembled aggregates and the magnetic field  $\mathbf{B}_0$  (i.e., the laboratory frame denoted by  $L$ ) according to:<sup>26</sup>

$$G^{\text{align}} = -\frac{1}{3} \Delta\chi^d B_0^2 \cdot \frac{1}{2} \langle 3 \cos^2 \theta_{\text{DL}} - 1 \rangle \quad (5)$$

Thus for a single domain of aggregates with  $\Delta\chi^d > 0$ , the free energy is minimized when the alignment of the domain director  $D$  is along the field direction  $L$  (i.e.,  $\theta_{\text{DL}} = 0^\circ$ ,  $D \parallel L$ ), whereas for domains possessing  $\Delta\chi^d < 0$ ,  $G^{\text{align}}$  is minimized when  $\theta_{\text{DL}} = 90^\circ$ ,  $D \perp L$ . For a collection of domains in a liquid crystal at equilibrium, perfect alignment with all directors  $D$

(26) de Gennes, P. G.; Prost, J. *The Physics of Liquid Crystals*, 2nd ed.; Clarendon Press: Oxford, 1993.

parallel ( $\Delta\chi^d > 0$ ) or perpendicular ( $\Delta\chi^d < 0$ ) to the applied magnetic field is in general unachievable, and we will use the notation  $\langle D \rangle \parallel L$  or  $\langle D \rangle \perp L$  to indicate that the angle  $\theta_{DL}$  is on average  $0^\circ$  or  $90^\circ$ :  $\langle \theta_{DL} \rangle = 0^\circ$  or  $\langle \theta_{DL} \rangle = 90^\circ$ , respectively.

Besides the thermal disordering induced by Brownian motions, viscous and/or elastic forces are also present that oppose the aligning torque produced by the magnetic field. The relative magnitudes of the opposing magnetic and viscoelastic forces dictate whether macroscopic alignment will occur and, if so, will also govern the rate at which the alignment process takes place. Due to the high viscosities and elasticities of most lyotropic liquid crystal phases, particularly those with high surfactant concentrations, magnetic alignment is often difficult to achieve over practical time scales (e.g., days), even in high fields (e.g., 11.7 T). A common procedure used to facilitate the creation of macroscopic alignment is to reduce the role of viscous and elastic forces by heating the liquid crystalline sample above its anisotropic–isotropic transition temperature. This is followed by a slow cooling through the transition where the temperature-dependent viscoelastic forces are reduced sufficiently, so that macroscopic alignment of re-nucleating liquid crystal domains can occur.

**$^2\text{H}$  NMR Simulations.** For an isotropic distribution of liquid crystalline domains, the  $^2\text{H}$  NMR line shape can be simulated by using the measured quadrupolar splitting of the Pake powder pattern in the experimental spectrum ( $\delta$ ) as an input parameter.<sup>20</sup> Similarly, the  $^2\text{H}$  NMR spectrum of an oriented sample can be simulated by using the same quadrupolar splitting of the Pake pattern as an input parameter, in addition to making assumptions about the form of the orientation distribution function. To quantify the extent of orientational ordering in each of the magnetic-field-aligned samples, a uniaxial Gaussian distribution of directors  $D$  about the average orientation  $\langle \theta_{DL} \rangle$  is often assumed,<sup>20</sup> with the full-width-at-half-maximum (fwhm) of this distribution function used as a second parameter. In the simulations presented below, macroscopic and microscopic uniaxiality (i.e., transverse isotropy) has been assumed, with the result that one angle,  $\theta_{DL}$ , suffices to specify the orientation distribution function  $P(\theta_{DL})$  as the fraction of director axes forming an angle between  $\theta_{DL}$  and  $\theta_{DL} + d\theta_{DL}$  with respect to the external magnetic field. For  $P(\theta_{DL})$ , a Gaussian distribution of aggregate directors is assumed:

$$P(\theta_{DL}) = N \exp\left(-\frac{(\theta_{DL} - \langle \theta_{DL} \rangle)^2}{2 \cdot \Delta\theta_{DL}}\right) \quad (6)$$

where  $\Delta\theta_{DL}$  specifies the fwhm of the distribution and  $N$  is a normalization constant. The average orientation  $\langle \theta_{DL} \rangle$  is determined by comparison of the experimental and simulated  $^2\text{H}$  NMR spectra, with  $\langle \theta_{DL} \rangle$  being either  $0^\circ$  or  $90^\circ$ , as previously discussed. In all cases, an appropriate Gaussian damping function is convoluted to account for spin–spin ( $T_2$ ) relaxation.<sup>27</sup> Furthermore, the uniqueness of the simulations is importantly verified by applying a  $90^\circ$  change in  $\langle \theta_{DL} \rangle$  and comparing the resulting calculated spectrum to the experimental spectrum obtained after a  $90^\circ$  rotation of the sample.

## Results and Discussion

The liquid crystalline properties of silicate–surfactant mesophases provide important opportunities for creating macroscopic

cally aligned materials because of their tendency to orient in applied magnetic fields.  $^2\text{H}$  NMR spectroscopy of deuterated surfactant species is a powerful *in situ* probe of phase morphology and the orientation distribution of silicate–surfactant liquid crystal domains. As discussed above, the orientation dependence of the  $^2\text{H}$  quadrupolar interaction, and thus the  $^2\text{H}$  NMR line shape, provides dynamical and structural information on lyotropic liquid crystals over molecular and macroscopic length scales that establish the primary factors governing orientational ordering of these complicated multicomponent systems in high magnetic fields. Applied to silicate–surfactant mesophases,  $^2\text{H}$  NMR line shape analyses allow the determination of the time-averaged local aggregate structures, the partitioning of surfactant molecules among different coexisting phases, the distribution of aggregate domain orientations relative to the applied magnetic field, and the diamagnetic susceptibilities of self-assembled aggregate domains.

For example, the  $^2\text{H}$  NMR spectrum shown in Figure 3a (left) of an initially unoriented silicate–surfactant mesophase displays a characteristic powder pattern with a 29.4 kHz quadrupolar splitting. This  $^2\text{H}$  splitting arises from a lamellar liquid crystalline morphology based on previous comparison of the molecular-level  $^2\text{H}$  NMR measurements with complementary experimental techniques that probe structure over longer length scales, such as small-angle X-ray diffraction and polarized optical microscopy.<sup>5</sup> For the example at hand, a lamellar morphology is expected, because the silicate–surfactant mesophase was prepared with hexanol added as a swelling agent to the mixture. Long- and medium-chain alcohols are known to facilitate the formation of lamellar lyotropic phases, because their hydrophilic –OH group imparts a degree of amphiphilic character to the molecules, whose small effective head groups thus favor morphologies with low aggregate curvatures.<sup>28</sup>

While strong magnetic fields can induce alignment of liquid crystals, the high viscoelasticity of silicate–surfactant liquid crystalline phases under ambient conditions prevents orientational ordering from occurring on time scales of weeks, even in an 11.7 T field. The alignment process, however, can be significantly accelerated by increasing the temperature. For example, an initially unoriented ensemble of lamellar silicate–surfactant mesophase domains becomes isotropic upon heating to  $95^\circ\text{C}$ , as evidenced by the collapse of the  $^2\text{H}$  NMR spectrum to the single narrow peak shown in Figure 3a (left, inset). Subsequent cooling of the sample through this isotropic–anisotropic transition in a 11.7 T magnetic field causes liquid crystal domains in the silicate–surfactant-rich phase to reform, but this time with a high degree of orientational order, according to the governing interactions imposed by the overall diamagnetic susceptibilities of the domains. This is clearly seen in the  $^2\text{H}$  NMR spectrum of Figure 3b, which shows a pair of sharp peaks and a small isotropic peak in the center of the spectrum. These correspond respectively to aligned silicate–surfactant liquid crystalline domains (whose orientation is discussed below) and an aqueous-rich isotropic phase, which coexist with one another. This thermal treatment through the anisotropic–isotropic transition, followed by re-nucleation of oriented domains in the presence of the applied magnetic field, was used to align all of the silicate–surfactant liquid crystal phases examined here: upon sufficient heating a random distribution of liquid crystalline domain orientations is converted to an isotropic phase, which subsequently reform aligned liquid crystal domains upon slow cooling in the magnetic field. The details of the alignment, however, are strongly dependent on the individual diamagnetic

(27) At  $25^\circ\text{C}$ , the  $^2\text{H}$  NMR spectrum reveals a slightly broader line width than the spectrum acquired at higher temperature. The increased line width at lower temperatures is due to shorter spin–spin ( $T_2$ ) relaxation times associated with reduced surfactant mobility. The  $T_2$  relaxation times were measured to be  $250 \pm 10$ ,  $660 \pm 10$ , and  $940 \pm 10 \mu\text{s}$  at 25, 40, and  $55^\circ\text{C}$ , respectively.

(28) Ekwall, P.; Mandell, L.; Fontell, K. *J. Colloid Interfac. Sci.* **1969**, 29, 639–646.

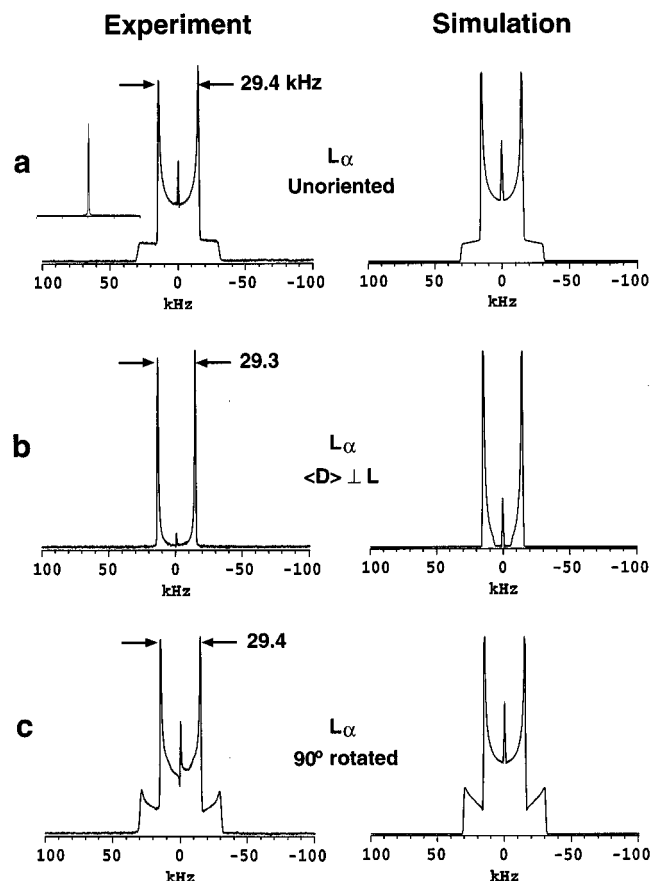


**Figure 3.** Experimental (left) and simulated (right)  $^2\text{H}$  NMR spectra of a lamellar ( $L_\alpha$ ) silicate–surfactant liquid crystal mixture with an overall molar composition of 1.6SiO<sub>2</sub>:186H<sub>2</sub>O:1.33TMAOH:0.50CTAB:15.8CH<sub>3</sub>OH:0.65CH<sub>3</sub>(CH<sub>2</sub>)<sub>5</sub>OH. Part a shows the experimental and simulated  $^2\text{H}$  NMR spectra for surfactant species in the as-made sample containing two phases, an unoriented lamellar silicate–surfactant-rich liquid crystal phase that accounts for the powder pattern with the 29.4 kHz splitting and an aqueous-rich phase that yields the narrow isotropic peak in the center. The simulated pattern was generated with 97% of CTA<sup>+</sup> species residing in randomly oriented lamellar domains and 3% in isotropic environments. As the sample is heated above its anisotropic–isotropic phase transition temperature (95 °C), a single narrow peak emerges, indicative of rapidly and isotropically mobile surfactant species in a sample lacking long-range or mesoscopic organization (left, inset). Part b shows the experimental  $^2\text{H}$  NMR spectrum (left) after heating the sample above its anisotropic–isotropic transition temperature and slow cooling in an 11.7 T magnetic field to align the lamellar domains. The simulated spectrum (b, right) is calculated with 97% of CTA<sup>+</sup> species in lamellar domains oriented on average perpendicular to the applied field ( $\langle D \rangle \perp L$ , Gaussian fwhm = 40°) and 3% in isotropic environments. Part c shows the experimental  $^2\text{H}$  NMR spectrum (left) that was obtained after rotating the sample in part b by 90° around an axis perpendicular to the magnetic field. The simulated spectrum (c, right) is obtained solely by applying a 90° rotation to the same parameters used in part b. The line shapes in both the experimental and simulated spectra are characteristic of an approximately planar distribution of domain directors. The good agreement between the experimental and simulated spectra in parts b and c confirms a *negative* overall domain susceptibility ( $\Delta\chi^d < 0$ ) and a perpendicular relationship between the domain directors and the applied magnetic field used to orient the sample in Figure 3b (i.e.,  $\langle \theta_{DL} \rangle = 90^\circ$ ). This situation is shown schematically in Figure 1a.

susceptibilities of the molecular components of the liquid crystal phase. Because of this, it is possible to tailor the alignment properties of a system, including the direction of orientational ordering, by controlling the constituent molecular components. Specific examples of such alignment control for lamellar and hexagonal liquid crystal phases are presented below.

**Aligned Lamellar Silicate–Surfactant Liquid Crystals.**  
**(a) Director Alignment ( $D$ )  $\perp$  Magnetic Field ( $B_0$ ):  $L_\alpha$  Phase with Hexanol.** The liquid crystalline properties of the silicate–surfactant mesophase shown in Figure 3a, as well as its lamellar morphology, have been previously established on the basis of  $^2\text{H}$  NMR line shape analyses and supported by X-ray diffraction and polarized optical microscopy measurements.<sup>5</sup> Quantitative comparison of the experimental  $^2\text{H}$  NMR spectrum and accompanying line shape simulations further allows the partitioning of deuterated surfactant species among different types of phase environments to be determined.<sup>21</sup> For example, the experimental  $^2\text{H}$  NMR spectrum in Figure 3a for a typical unaligned silicate–CTA<sup>+</sup> mesophase is compared with a simulated line shape containing a superposition of well-resolved spectral contributions from different well-defined morphological elements. The individual intensities associated with each such element can be varied to match the experimental spectrum. In this way, the heterogeneous sample of Figure 3a is determined to consist of two phases: (i) a collection of randomly distributed lamellar domains containing 97% of the CTA<sup>+</sup> surfactant molecules ( $\Delta\nu = 29.4$  kHz), and (ii) a highly mobile isotropic component accounting for 3% of the CTA<sup>+</sup> species that remain dissolved in the aqueous-rich phase.

Similarly, surfactant partitioning among different environments in aligned liquid crystalline materials can be determined from  $^2\text{H}$  NMR line shape analyses, which additionally quantify the degree of orientational order present. For example, after aligning the hexanol-containing lamellar silicate–surfactant mesophase sample (Figure 3a), the experimental and simulated  $^2\text{H}$  NMR spectra in Figure 3b establish that 97% of the CTA<sup>+</sup> molecules reside in oriented lamellar domains ( $\Delta\nu = 29.3$  kHz, with a 35° fwhm Gaussian distribution), with the remainder (3%) occupying isotropic environments in the H<sub>2</sub>O-rich phase. On the basis of eq 1, the 29.3 kHz  $^2\text{H}$  splitting ascribed to the oriented liquid crystal fraction reflects mean alignment of the directors  $D$  of the lamellar domains perpendicular to the direction of the applied 11.7 T magnetic field, i.e.,  $\langle D \rangle \perp L$  or  $\langle \theta_{DL} \rangle = 90^\circ$ . As shown schematically in Figure 1a, such an orientation corresponds to an approximately planar distribution of domain directors in the azimuthal direction. This can be verified by rotating the sample container through a known discrete angle, acquiring a new  $^2\text{H}$  NMR spectrum, and subsequently comparing it with that predicted by using the same simulation parameters determined in Figure 3b modified solely by the rotation angle imposed. For example, a 90° rotation of the sample with respect to the applied magnetic field yields the experimental  $^2\text{H}$  NMR spectrum shown in Figure 3c, left ( $\Delta\nu = 29.4$  kHz). This experimental spectrum displays a distribution of signal intensity that is distinct in important ways from the powder pattern (Figure 3a) produced by a fully random distribution of domain directors. The simulated spectrum in Figure 3c (right) assumes a planar distribution of domain directors with respect to the  $B_0$  field in the rotated sample, which verifies the approximately planar distribution of domain directors in the original magnetic field-aligned sample (Figure 3b). The excellent agreement between the experimental and simulated spectra in Figures 3b and 3c indicates a self-consistent set of simulation parameters, which provides a high degree of confidence in the quantitative alignment measurements.

The orientational ordering of the liquid crystal domains in this lamellar silicate–surfactant mesophase can be understood in terms of the molecular diamagnetic susceptibilities of the material's constituent species. First of all, by using  $\langle \theta_{DL} \rangle = 90^\circ$  (from Figure 3b) and minimizing the angle-dependent free energy (i.e.,  $G^{\text{align}} < 0$ ) in eq 5, the overall diamagnetic

susceptibility of the lamellar silicate–surfactant mesophase domains must be  $\Delta\chi^d < 0$ . This arises from the negative diamagnetic susceptibilities of the individual CTA<sup>+</sup> species<sup>29</sup> and hexanol molecules ( $\Delta\chi^m < 0$ ) from which the aggregates are formed. Because the CTA<sup>+</sup> and hexanol molecular axes ( $M_s$  and  $M_h$ ) are parallel to the lamellar director ( $D$ , Figure 1a), the term  $\langle 3 \cos^2 \theta_{MD} - 1 \rangle_D$  in eq 4 is positive. Thus, the molecular and domain diamagnetic susceptibilities must possess the same sign, in this case negative, to fulfill the thermodynamic requirement that  $G^{\text{align}} < 0$ . The CTA<sup>+</sup> and hexanol species thus satisfy their respective minimum energy configurations by adopting common orientations perpendicular to the  $B_0$  magnetic field, with the result that the director axes of the planar aggregates also align perpendicular to the direction of the magnetic field. Such is also the case for ternary CTAB/H<sub>2</sub>O/decanol systems, where disk-like bilayers become macroscopically oriented with their normal axes perpendicular to an orienting magnetic field (i.e.,  $\Delta\chi^d < 0$ ).<sup>30</sup> The similar orientational ordering behavior for the multicomponent silicate–surfactant and ternary CTAB/H<sub>2</sub>O/decanol mixtures indicates that the exchange of Br<sup>−</sup> anions for multiply charged silicate anions does not alter the sign of the overall diamagnetic susceptibilities of the planar aggregates and lamellar domains, which align with their plane-normal director axes perpendicular to the magnetic field in both liquid crystal systems.

**(b) Director Alignment ( $D$ ) || Magnetic Field ( $B_0$ ):  $L_\alpha$  Phase with Benzene.** Significant control over the orientational ordering behavior of silicate–surfactant liquid crystals can be exerted by choosing the constituent chemical species according to their diamagnetic susceptibilities. For example, different lamellar alignments can be achieved by selecting organic solute molecules with different diamagnetic susceptibilities and thus different orienting properties in magnetic fields. Instead of hexanol, benzene can also be used as a swelling agent to favor the formation of a lamellar silicate–surfactant mesophase:<sup>24</sup> by incorporating either additive into the hydrophobic regions of a lyotropic liquid crystal material, morphologies with reduced local curvatures are favored. The experimental <sup>2</sup>H NMR spectrum and simulated line shape for an unoriented lamellar silicate–surfactant mesophase formed with benzene are shown in Figure 4a. Similar results are observed for the partitioning of surfactant molecules between the liquid crystal and isotropic phases, as found for the lamellar mesophase prepared with hexanol: (i) 98% of the  $\alpha$ -deuterated CTA<sup>+</sup> species are in randomly oriented lamellar domains in the silicate–surfactant-rich phase ( $\Delta\nu = 27.7$  kHz), and (ii) 2% are highly mobile in isotropic environments in the aqueous-rich phase.

After aligning this benzene-containing lamellar silicate–surfactant mesophase according to the same thermal/magnetic-field procedure described above, the resulting <sup>2</sup>H NMR spectrum shown in Figure 4b is dominated by a doublet with a splitting of 55.9 kHz, with a less pronounced powder pattern ( $\Delta\nu = 27.6$  kHz) and a small isotropic peak as secondary features. The accompanying simulated spectrum indicates that 78% of the CTA<sup>+</sup> molecules reside in lamellar domains in which the planar aggregate directors are oriented on average *parallel* to the magnetic field ( $\Delta\nu = 55.9$  kHz,  $\langle D \rangle || L$  or  $\langle \theta_{DL} \rangle = 0^\circ$  with a 50°-fwhm Gaussian distribution, Figure 1b), 20% belong to randomly oriented lamellar domains ( $\Delta\nu = 27.6$  kHz), and 2% are rapidly mobile in the aqueous-rich phase. The significant fraction of randomly oriented CTA<sup>+</sup> species in this material arises from disorder that is quenched into the viscoelastic systems as the liquid crystal domains nucleate and grow during

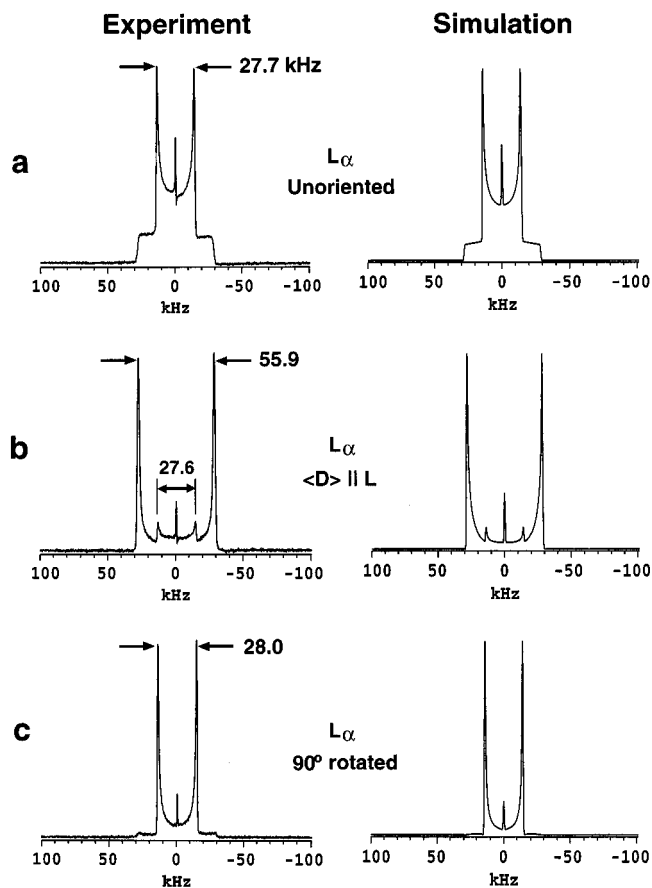


**Figure 4.** Experimental (left) and simulated (right) <sup>2</sup>H NMR spectra of a lamellar ( $L_\alpha$ ) silicate–surfactant liquid crystal mixture with an overall molar composition of 1.6SiO<sub>2</sub>:209H<sub>2</sub>O:1.33TMAOH:0.50CTAB:15.7CH<sub>3</sub>OH:2.2C<sub>6</sub>H<sub>6</sub>. For the as-made sample in part a, comparison of the experimental and simulated patterns indicates that 98% of the CTA<sup>+</sup> species belong to randomly oriented lamellar domains (27.7 kHz splitting) and 2% are highly mobile in isotropic environments. Part b shows the experimental <sup>2</sup>H NMR spectrum (left) after aligning the sample in an 11.7-T magnetic field. The simulated spectrum (b, right) is calculated by assigning 77% of the CTA<sup>+</sup> species to lamellar domains oriented parallel to the applied field ( $\langle D \rangle || L$ , Gaussian fwhm = 50°), 20% to randomly oriented lamellar domains, and 3% to rapidly mobile isotropic environments. Part c shows the <sup>2</sup>H NMR spectrum that was obtained after rotating the sample in part b by 90° around an axis perpendicular to the magnetic field. The simulated spectrum (part c, right) is obtained solely by applying a 90° rotation to the same parameters used in part b. Close agreement between the experimental and simulated spectra in parts b and c verifies a *positive* overall domain diamagnetic susceptibility ( $\Delta\chi^d > 0$ ) and a parallel relationship between the domain directors and the applied magnetic field used to orient the sample in Figure 4b (i.e.,  $\langle \theta_{DL} \rangle = 0^\circ$ ). This situation is shown schematically in Figure 1b.

the slow cooling process. Following a 90° rotation of the sample with respect to the applied magnetic field, subsequent experimental ( $\Delta\nu = 28.0$  kHz) and simulated <sup>2</sup>H NMR spectra shown in Figure 4c confirm the domain orientations and their distributions, which are thus without ambiguity. Thus, the mean orientation of the aligned lamellar silicate–surfactant mesophase prepared with benzene as an organic additive (Figure 4b) is offset by 90° from that of the lamellar system prepared with hexanol (Figure 3b) in otherwise equivalent mixtures. This demonstrates the feasibility of manipulating macroscopic orientational order in silicate–surfactant liquid crystal systems by adjusting mixture composition to achieve a desired field-alignment response.

The significantly different orientational ordering behavior of benzene- and hexanol-containing lamellar silicate–CTA<sup>+</sup> liquid

(29) Hertel, G.; Hoffmann, H. *Liq. Cryst.* **1989**, *5*, 1883–1898.

(30) Hertel, G.; Hoffmann, H. *Prog. Colloid Polym. Sci.* **1988**, *76*, 123–131.

crystals is easily explained by the different magnetic-field alignment properties of the two organic additives in the confined aggregate environments. By using the measured quadrupolar splitting in Figure 4b in conjunction with eqs 1 and 5, a positive diamagnetic susceptibility (i.e.,  $\Delta\chi^d > 0$ ) is established for the lamellar domains containing benzene, with the normal directors of the planar aggregates oriented on average parallel to the magnetic field ( $\langle D \rangle \parallel L$ ), as illustrated schematically in Figure 1b. The overall positive diamagnetic susceptibility of these planar aggregates and the corresponding self-assembled lamellar domains requires the long molecular axes (i.e., the alkyl chains) of the silicate–CTA<sup>+</sup> species to be parallel to the orienting magnetic field. As discussed above, this configuration of the CTA<sup>+</sup> species alone is unfavorable, because the diamagnetic susceptibilities of the individual surfactant molecules are negative. However, the use of benzene (in a molar ratio benzene/CTA<sup>+</sup>  $\geq 3.5$ ) instead of hexanol to stabilize the lamellar silicate–surfactant mesophase has an important influence on the orientational ordering behavior of the planar aggregates. Aromatic molecules are known to display strong positive diamagnetic susceptibilities, with the planes of the aromatic rings orienting parallel (i.e., coplanar) to an applied magnetic field.<sup>31</sup> Consequently, the large positive susceptibilities ( $\Delta\chi^m > 0$ ) of the benzene molecules overcome the smaller negative molecular susceptibilities ( $\Delta\chi^m < 0$ ) of the alkyl components associated with the silicate–CTA<sup>+</sup> species to produce an overall positive diamagnetic susceptibility ( $\Delta\chi^d > 0$ ) for the lamellar silicate–surfactant liquid crystal domains that contain benzene. Therefore, for the mixture composition used, the benzene solute molecules exert a dominant influence on the orientational ordering of the lamellar silicate–CTA<sup>+</sup> mesophase domains. Furthermore, due to steric constraints, the benzene molecules are expected to orient parallel to the surfactant chains to pack most efficiently with the CTA<sup>+</sup> species.<sup>32,33</sup> This geometry corresponds to a parallel relationship between the molecular axes of the surfactant species and the planes of the benzene molecules,  $M_s$  and  $M_b$ , respectively, as illustrated schematically in Figure 1b. The positive diamagnetic susceptibility of the lamellar liquid crystal domains in this sample is consistent with the benzene molecules adopting orientations parallel to the surfactant alkyl chains in the hydrophobic regions of the aggregates.

#### Aligned Hexagonal Silicate–Surfactant Liquid Crystals.

**(a) Director Alignment ( $D$ )  $\parallel$  Magnetic Field ( $B_0$ ):  $H_\alpha$  Phase with No Organic Additives.** It is possible to extend the understanding of how molecular diamagnetic susceptibilities ( $\Delta\chi^m$ ) influence the overall domain diamagnetic susceptibilities ( $\Delta\chi^d$ ) of multicomponent silicate–surfactant liquid crystals to predict and thereby control the mesoscopic orientational ordering behavior of other silicate–surfactant mesophases in high magnetic fields. For example, hexagonal silicate–surfactant mesophases result when CTAB alone is used as the amphiphilic structure-directing species in the absence of other organic additives.<sup>5,6</sup> As portrayed schematically in Figure 2a, the hexagonal morphology results in surfactant configurations where the CTA<sup>+</sup> molecular axes ( $M_s$ ) and aggregate director ( $D$ ) are perpendicular to each other (i.e.,  $\theta_{MD} = 90^\circ$ ), and thus the term  $\langle 3 \cos^2 \theta_{MD} - 1 \rangle_D$  in eq 4 is negative. As a result, the surfactant

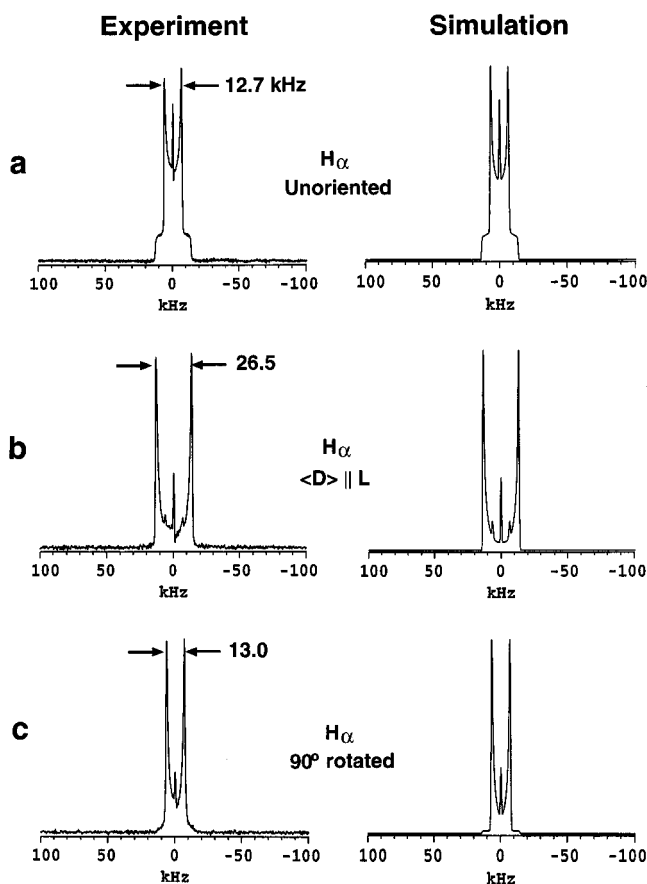


**Figure 5.** Experimental (left) and simulated (right)  $^2\text{H}$  NMR spectra of a hexagonal ( $H_\alpha$ ) silicate–surfactant liquid crystal mixture with an overall molar composition of 1.6SiO<sub>2</sub>:209H<sub>2</sub>O:1.33TMAOH:0.50CTAB:15.7CH<sub>3</sub>OH. The experimental and simulated patterns shown in part a indicate that 96% of the CTA<sup>+</sup> species belong to randomly oriented hexagonal domains (12.7 kHz splitting) and 4% are highly mobile in isotropic environments. Part b shows the experimental  $^2\text{H}$  NMR spectrum (left) acquired after aligning the sample in an 11.7 T magnetic field. The simulated spectrum (b, right) is calculated for 60% of CTA<sup>+</sup> species in hexagonal domains oriented parallel to the applied field ( $\langle D \rangle \parallel L$ , Gaussian fwhm = 50°), 35% in randomly oriented hexagonal domains, and 5% in rapidly mobile isotropic environments. Part c shows the experimental  $^2\text{H}$  NMR spectrum (left) that was acquired after rotating the sample in part b by 90° around an axis perpendicular to the applied field. The simulated spectrum (part c, right) is obtained solely by applying a 90° rotation to the same parameters used in part b. The good agreement between the experimental and simulated spectra in parts b and c verifies a *positive* overall domain diamagnetic susceptibility ( $\Delta\chi^d > 0$ ) and a parallel relationship between the domain directors and the applied field used to orient the sample in Figure 5b (i.e.,  $\langle \theta_{DL} \rangle = 0^\circ$ ). This situation is shown schematically in Figure 2a.

molecular ( $\Delta\chi^m$ ) and domain ( $\Delta\chi^d$ ) diamagnetic susceptibilities of hexagonal silicate–CTA<sup>+</sup> liquid crystals are of opposite signs. As discussed above for the lamellar materials, CTAB has a negative molecular diamagnetic susceptibility ( $\Delta\chi^m < 0$ ), so that hexagonal silicate–surfactant domains containing CTA<sup>+</sup> without organic additives will possess a positive overall diamagnetic susceptibility ( $\Delta\chi^d > 0$ ), which will cause the domains to align parallel to an applied magnetic field.

Confirmation of the predicted alignment and diamagnetic susceptibility properties of hexagonal silicate–surfactant mesophases is established by following the same procedure used for the lamellar mesophase systems described above. Figure 5a (left) shows the experimental room temperature  $^2\text{H}$  NMR spectrum of an unoriented silicate–surfactant liquid crystal possessing a hexagonal morphology. Comparison with the

(31) de Jeu, W. H. *Physical Properties of Liquid Crystalline Materials*; Gordon and Breach Science Publishers: New York, 1979; p 32.

(32) Kilpatrick, P. K.; Blackburn, J. C.; Walter, T. A. *Langmuir* **1992**, *8*, 2192–2199.

(33) The location of solubilized benzene molecules in the palisade region of the aggregates (i.e., near the hydrophilic–hydrophobic interface) is supported by  $^2\text{H}$  NMR measurements by using deuterated benzene. The residual  $^2\text{H}$  quadrupolar splitting was measured to be 4.6 kHz, indicative of a highly anisotropic motional averaged environment.<sup>22</sup>

accompanying simulated spectrum (Figure 5a, right) establishes that the sample is comprised of a mixture in which 97% of the CTA<sup>+</sup> species are in randomly oriented hexagonal domains ( $\Delta\nu = 12.7$  kHz), with the remaining 3% accounting for the narrow peak in the center of the spectrum, attributed to isotropically mobile surfactant molecules in the aqueous-rich phase.

Figure 5b shows the experimental and simulated <sup>2</sup>H NMR spectra of the same hexagonal silicate–surfactant mesophase, following thermal treatment and slow cooling of the sample through its isotropic–anisotropic transition in an 11.7 T magnetic field. In this aligned sample, 87% of the CTA<sup>+</sup> species belong to hexagonal domains in which the longitudinal aggregate axes are oriented on average *parallel* to the applied magnetic field ( $\Delta\nu = 26.5$  kHz,  $\langle D \rangle \parallel L$  or  $\langle \theta_{DL} \rangle = 0^\circ$  with a 40° fwhm Gaussian distribution, Figure 2a), 10% CTA<sup>+</sup> species reside in randomly oriented hexagonal domains (low intensity powder pattern with  $\Delta\nu = 12.7$  kHz), and the remainder (3%) occupy isotropic environments in the H<sub>2</sub>O-rich phase.

The parallel orientation of the majority of the hexagonal domains with respect to the applied field establishes the overall positive diamagnetic susceptibility for the cylindrical aggregates and corresponding hexagonal domains ( $\Delta\chi^d > 0$ , eq 5). Figure 5c (left) shows the experimental <sup>2</sup>H NMR spectrum of the sample after a rotation of 90° with respect to the magnetic field, along with a simulated spectrum (Figure 5c, right) produced by using the same parameters as determined in Figure 5b modified only to account for the rotated field orientation. The excellent agreement between the experimental and simulated spectra b and c in Figure 5 confirms the corresponding surfactant partitioning within the heterogeneous silicate–CTA<sup>+</sup> sample, the positive diamagnetic susceptibility for the hexagonal domains ( $\Delta\chi^d > 0$ ) in the absence of organic additives, and the preference of the hexagonal domains to orient with their director axes parallel to the applied magnetic field.

**(b) Director Alignment (*D*) ⊥ Magnetic Field (*B*<sub>0</sub>): H<sub>α</sub> Phase with Benzene.** To establish unambiguously the role of aromatic additives like benzene on the magnetic-field-induced alignment of silicate–surfactant liquid crystal phases, a similar set of measurements was performed on the hexagonal material of Figure 5 to which a small amount of benzene had been added. It has previously been found that the hexagonal phase of these materials remains stable with respect to the lamellar phase for low benzene concentrations (e.g., molar ratios benzene/CTA<sup>+</sup> < 2.3).<sup>5</sup> For example, addition of 0.2 wt % benzene to a mixture that is otherwise identical with the hexagonal liquid crystal material of Figure 5 does not affect the system's hexagonal mesoscopic morphology, as shown by the room temperature <sup>2</sup>H NMR spectrum in Figure 6a for an unoriented sample. The silicate–CTA<sup>+</sup> H<sub>α</sub> phase displays a quadrupolar splitting of 13.2 kHz, with the accompanying simulations establishing that 97% of the CTA<sup>+</sup> species belong to randomly oriented hexagonal domains, while 3% experience rapid isotropic mobility in the aqueous-rich phase. After alignment in the 11.7 T magnetic field (Figure 6b, left), the spectrum is now seen to possess intensity that is concentrated at the singularities ( $\Delta\nu = 13.1$  kHz) corresponding to hexagonal domains whose aggregate axes are aligned on average perpendicular to the applied magnetic field,  $\langle D \rangle \perp L$  or  $\langle \theta_{DL} \rangle = 90^\circ$ . Again, the simulated spectrum (Figure 6b, right) establishes this quantitatively: 77% of the surfactant molecules reside in hexagonal domains oriented perpendicular to the magnetic field (Gaussian fwhm = 40°), 20% are in randomly oriented hexagonal domains, and 3% are highly mobile in isotropic environments.

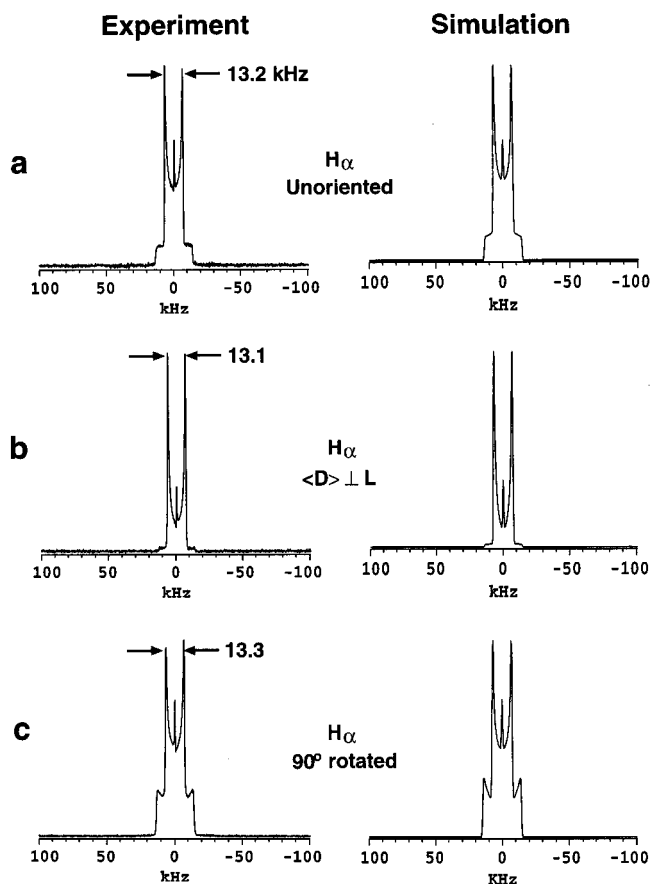


**Figure 6.** Experimental (left) and simulated (right) <sup>2</sup>H NMR spectra of a hexagonal (H<sub>α</sub>) silicate–surfactant liquid crystal mixture with an overall molar composition of 1.6SiO<sub>2</sub>:209H<sub>2</sub>O:1.33TMAOH:0.50CTAB:15.7CH<sub>3</sub>OH:0.6C<sub>6</sub>H<sub>6</sub>. The experimental and simulated patterns shown in part a for the as-made sample indicate that 97% of the CTA<sup>+</sup> species belong to randomly oriented hexagonal domains (13.2 kHz splitting) and 3% to highly mobile isotropic environments. Part b shows the experimental <sup>2</sup>H NMR spectrum (left) obtained after aligning the sample in an 11.7 T magnetic field. The simulated spectrum (part b, right) is calculated for 75% of the CTA<sup>+</sup> species residing in hexagonal domains oriented perpendicular to the applied field ( $\langle D \rangle \perp L$ , Gaussian fwhm = 40°), 20% in randomly oriented hexagonal domains, and 5% in isotropic environments. Part c shows the experimental <sup>2</sup>H NMR spectrum (left) that was obtained after rotating the sample used in part b by 90° around an axis perpendicular to the applied field. This spectra again shows an approximately planar distribution of domain directors. The simulated spectrum (part c, left) is obtained solely by applying a 90° rotation to the same parameters used in part b. The good agreement between the experimental and simulated spectra in parts b and c confirms the overall *negative* domain susceptibility ( $\Delta\chi^d < 0$ ) and a perpendicular relationship between the aligned domain directors and the applied field used to orient the sample in Figure 6b (i.e.,  $\langle \theta_{DL} \rangle = 90^\circ$ ). This situation is shown schematically in Figure 2b.

As discussed in the context of the lamellar phase in Figure 4 above, local steric constraints are expected to cause a significant quantity of the benzene solute molecules to orient parallel to the surfactant alkyl chains in the hexagonal-phase aggregates. Consideration of the time averaging of both local and translational motions of the benzene molecules, in combination with their dominant molecular diamagnetic susceptibility  $\Delta\chi^m > 0$ , yields an overall negative susceptibility ( $\Delta\chi^d < 0$ , eqs 4 and 5) for the corresponding hexagonal mesophase domains. Furthermore, the <sup>2</sup>H NMR spectrum and accompanying simulation (Figure 6c) of the oriented sample acquired after its rotation through 90° affirms an approximately planar distribution of domain directors in the transverse plane before rotation (Figure 6b) and in the field plane afterward. The excellent agreement

between the experimental and simulated spectra b and c in Figure 6 establishes unambiguously the overall negative diamagnetic susceptibility of this benzene-containing hexagonal silicate–surfactant mesophase and confirms the role of individual molecular additives in controlling the orientational ordering properties of these systems.

**Phase Transitions between Aligned Silicate–Surfactant Mesophases.** The alignment of mesophase domains and the distribution of their collective orientations can be used to gain insight into the nature of phase transitions between two mesoscopically ordered morphologies. It has previously been shown that organic solutes, such as trimethylbenzene, benzene, or hexanol, stabilize lamellar silicate–surfactant mesophases because of their higher solubility within the hydrophobic regions of the aggregates.<sup>5–7</sup> Upon heating such lamellar liquid crystals, however, the diminished relative solubilities of organic additives in the hydrophobic aggregate cores result in their expulsion into the aqueous-rich phase. This produces increased curvature at the silicate–surfactant interface that can ultimately contribute to a first-order transformation to a hexagonal morphology.<sup>5</sup> Upon cooling to room temperature in the absence of silica polymerization, the solute molecules are reincorporated into the hydrophobic regions of the aggregates, with the result that the sample morphology reversibly converts back to the original lamellar structure. The direct correlation between the lamellar/hexagonal mesophase transitions and the expulsion/reincorporation of the organic solute in these systems has been previously established.<sup>5</sup> This is useful to the present study, which can exploit the enhanced resolution of  $^2\text{H}$  NMR spectra of aligned silicate–surfactant liquid crystals to examine transformations between magnetic-field-aligned lamellar and hexagonal morphologies. By understanding the molecular origin of orientational ordering in silicate–surfactant mesophases and by utilizing the magnetic field alignment techniques discussed above, we explore in detail the temperature-induced structural transformations between ordered mesophases.

As an initially unoriented lamellar silicate–surfactant mesophase sample containing benzene (see Figure 7a,  $\Delta\nu = 28.0$  kHz) is heated from room temperature through its anisotropic–isotropic phase transition, an isotropic  $^2\text{H}$  NMR signal emerges (see Figure 7b), as discussed previously. As the sample is cooled slowly within a 11.7 T magnetic field, a quadrupolar doublet first emerges at approximately 75 °C. The 11.3 kHz splitting of the  $^2\text{H}$  NMR spectrum acquired at 70 °C (see Figure 7c) arises from the formation of an oriented hexagonal silicate–CTA<sup>+</sup> liquid crystal with its director axes aligned perpendicular to the applied magnetic field (i.e.,  $\langle D \rangle \perp L$  or  $\langle \theta_{DL} \rangle = 90^\circ$  with a 40° fwhm Gaussian distribution; see also Figure 6b). As the temperature is gradually reduced from 70 to 45 °C, the phase behavior of this system becomes more complex. The 12.1 kHz splitting associated with the hexagonal phase reflects increased local ordering at the lower temperature, consistent with the expected increase of the order parameter  $S_{CD}$  as the temperature is reduced. In addition, however, a second coexisting equilibrium phase appears, as evidenced by the 52.7 kHz splitting observed in Figure 7d. This 52.7 kHz splitting reflects a lamellar morphology whose domain directors are on average oriented parallel to the applied magnetic field  $\langle D \rangle \parallel L$  or  $\langle \theta_{DL} \rangle = 0^\circ$ , as similarly observed in Figure 4b. These phases and their corresponding orientations have been confirmed by separate 90° sample rotations and simulations (not shown here).<sup>22</sup>

As the temperature is further reduced to 25 °C, the  $^2\text{H}$  NMR spectrum in Figure 7e reveals that the macroscopically ordered lamellar mesophase persists (with a small isotropic fraction) as the hexagonal phase disappears entirely. The transient response

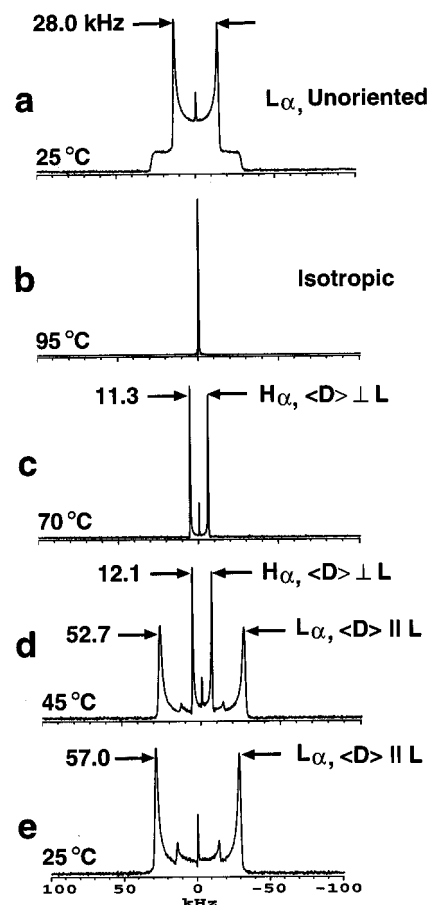


**Figure 7.** Experimental  $^2\text{H}$  NMR spectra of a silicate–surfactant liquid crystal mixture with an overall molar composition of 1.6SiO<sub>2</sub>:209H<sub>2</sub>O:1.33TMAOH:0.50CTAB:15.7CH<sub>3</sub>OH:2.2C<sub>6</sub>H<sub>6</sub> (same as in Figure 4). Part a shows the room temperature spectrum for surfactant species in the as-made sample containing two phases, an unoriented lamellar silicate–surfactant-rich liquid crystal phase, which accounts for the powder pattern with the 28.0 kHz splitting, and an aqueous-rich phase, which yields the narrow isotropic peak in the center. Part b shows the  $^2\text{H}$  NMR spectrum acquired after heating the sample above its anisotropic–isotropic transition temperature (95 °C), which produces a single sharp isotropic peak. After the sample was cooled to 70 °C in an 11.7 T field, the spectrum in part c displays features from highly aligned hexagonal domains whose directors are on average oriented perpendicular to the applied field ( $\Delta\nu = 11.3$  kHz,  $\langle \theta_{DL} \rangle = 90^\circ$ , Gaussian fwhm = 40°) and a coexisting aqueous-rich isotropic phase. At 45 °C, the spectrum in part d reflects the coexistence of three phases: hexagonal domains with  $\langle D \rangle \perp L$  ( $\Delta\nu = 12.1$  kHz), lamellar domains with  $\langle D \rangle \parallel L$  ( $\Delta\nu = 52.7$  kHz), and the H<sub>2</sub>O-rich isotropic phase. The room temperature spectrum in part e consists of components from the aqueous-rich isotropic phase and a lamellar silicate–surfactant mesophase; 75% of the CTA<sup>+</sup> species belong to lamellar domains that are oriented with their aggregate directors on average parallel to the magnetic field ( $\Delta\nu = 57.0$  kHz), and 22% reside in randomly oriented domains ( $\Delta\nu = 27.9$  kHz).

of the system to the temperature changes, as monitored by  $^2\text{H}$  NMR, suggests a gradual transformation between these two magnetic-field-oriented morphologies. The microscopic nature of the observed transformation between a hexagonal phase with  $\langle D \rangle \perp L$  (see Figure 2b) and a lamellar phase with  $\langle D \rangle \parallel L$  (see Figure 1b) appears to occur through fusion of neighboring cylindrical aggregates in orientations that satisfy the overall magnetic susceptibility of the resulting planar domains. Because the transition temperature is too low (and thus the viscosity and/or elasticity too high) to allow for macroscopic reorientation of the resulting lamellar domains, this epitaxial relationship<sup>34</sup> between the aligned hexagonal and aligned lamellar domains

**Table 1.** Summary of the Orientational Ordering Behavior of Lamellar and Hexagonal Silicate–Surfactant Liquid Crystals Formed by Using Organic Species with Different Molecular Diamagnetic Susceptibilities  $\Delta\chi^m$ <sup>a</sup>

figure no.	phase	surfactant/ swelling agent	$\Delta\chi^m$	$\langle 3 \cos^2 \theta_{MD} - 1 \rangle_D$	$\Delta\chi^d$ (eq 4)	$(3 \cos^2 \theta_{DL} - 1)$ (eq 5)	$\langle \theta_{DL} \rangle$
3	L <sub>α</sub>	CTA <sup>+</sup> /hexanol	–	+	–	–	90°
4	L <sub>α</sub>	CTA <sup>+</sup> /benzene	+	+	+	+	0°
5	H <sub>α</sub>	CTA <sup>+</sup> /none	–	–	+	+	0°
6	H <sub>α</sub>	CTA <sup>+</sup> /benzene	+	–	–	–	90°

<sup>a</sup>The entries under  $\Delta\chi^m$  represent summed quantities. Depending on the mesophase composition, either positive or negative domain diamagnetic susceptibilities ( $\Delta\chi^d$ ) can be obtained, allowing control over the direction of mesophase alignment  $\langle \theta_{DL} \rangle$  in an applied magnetic field.

is important for explaining the oriented-hexagonal to oriented-lamellar transformation. We note that, while fusion of neighboring cylindrical aggregates could produce lamellar domains with any orientation with respect to the applied field, only those domains in energetically favorable  $\langle \theta_{DL} \rangle = 0^\circ$  configurations are observed to form, demonstrating that the applied field can break the degeneracy of the originally multidimensional potential surface of the phase transition.

In addition, the original orientation distribution of the hexagonal domains (see Figure 7c) manifests itself in the resulting orientation distribution of the lamellar mesophase: the corresponding <sup>2</sup>H NMR spectrum in Figure 7e of the oriented lamellar phase can be simulated (not shown here) with 75% of the CTA<sup>+</sup> molecules residing in lamellar domains in which the planar aggregate directors are oriented on average parallel to the magnetic field ( $\Delta\nu = 57.0$  kHz,  $\langle D \rangle \parallel L$  or  $\langle \theta_{DL} \rangle = 0^\circ$  with a 50° fwhm Gaussian distribution, Figure 1b), 22% belonging to randomly oriented lamellar domains ( $\Delta\nu = 27.9$  kHz), and 3% rapidly mobile in the aqueous-rich phase. The finite fraction ( $\approx 20\%$ ) of randomly oriented lamellar domains appears to be typical in systems where the oriented lamellar mesophase is produced through an intermediate oriented hexagonal morphology (e.g., Figures 4b and 7b), and is not observed in oriented lamellar systems that form directly from the viscous isotropic phase (e.g., Figure 3). Furthermore, the similarities observed for the partitioning of domain orientation distributions in the final lamellar phase (75% aligned and 22% randomly oriented L<sub>α</sub>) and that in benzene-containing hexagonal phases (77% aligned and 20% randomly oriented H<sub>α</sub>) are consistent with the epitaxial nature of the phase transition. If the transition were to proceed through a nonepitaxial nucleation and growth mechanism, no correlation would be expected between the distributions of hexagonal and lamellar domain orientations.

More detailed analyses of the resultant <sup>2</sup>H NMR quadrupolar splittings in Figure 7 and of other silicate–surfactant mesophases can be used to obtain specific information on the local structure and dynamics of the surfactant species under different mixture conditions. For instance, the temperature-dependent local order parameters ( $S_{CD}$ ) of magnetic-field-aligned and powder samples containing lamellar and/or hexagonal phases can be determined by using eqs 1 and 3, respectively. The variation of the local order parameter with temperature for a number of different mixture compositions is shown in Figure 8. The decrease of  $S_{CD}$  with increasing temperature corresponds to higher local molecular mobilities of the aliphatic chain and is common to all liquid crystalline materials.<sup>16a,35</sup> In addition, for all alkaline silicate–surfactant liquid crystal compositions thus far examined, the local order parameters of surfactant molecules residing

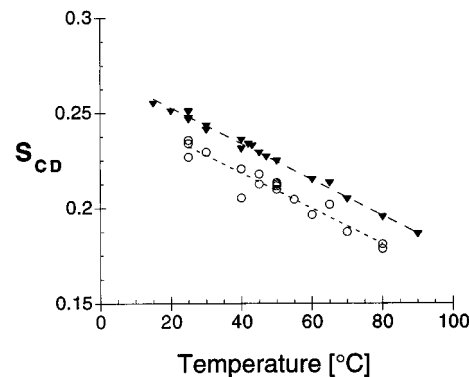


**Figure 8.** The local order parameter ( $S_{CD}$ ) of the C–<sup>2</sup>H bonds in various lamellar (▼) and hexagonal (○) silicate–surfactant mesophases as a function of temperature. The straight lines have been added to guide the eye. For both the lamellar and hexagonal mesophases,  $S_{CD}$  decreases with increasing temperature, indicating that local ordering decreases as molecular mobility increases.

in the cylindrical aggregates of the hexagonal phase are smaller than those confined within the planar sheets of the lamellar phase. This observation is consistent with the generally larger head group area  $a_0$  available to the surfactant molecules residing at a curved surface.<sup>14b,28</sup> As the temperature is further increased to a point where anisotropic–isotropic phase transitions (i.e., melting) take place, the quadrupolar splittings vanish abruptly, resulting in narrow peaks in the corresponding <sup>2</sup>H NMR spectra.

The distributions and alignments of the observed phases in Figures 7 and 8 are completely reversible with respect to temperature and do not change with time, indicating that the system is at thermal equilibrium for each temperature shown. At a given silicate–surfactant mixture composition and temperature (and in the absence of silica polymerization), a variety of morphologies can therefore coexist in equilibrium.

**Silicate–Surfactant Mesophase Stability.** For all of the lamellar and hexagonal silicate–surfactant mesophases discussed above, the high viscosity/elasticity at room temperature renders reorientation of the liquid crystalline domains negligible on time scales much longer than the <sup>2</sup>H NMR measurements at 11.7 T. Similarly, removal of the oriented samples at room temperature from the 11.7 T magnetic field resulted in no detectable disordering of aggregate or domain orientations over periods of at least 6 months. After such periods, the <sup>2</sup>H NMR spectra of the oriented samples remained unchanged,<sup>22</sup> indicating that the time scales are very long for thermal relaxation of the oriented domains toward a random distribution. The high viscoelasticities of silicate–surfactant mesophases at room temperature apparently hinder restoration of the initially aligned liquid crystalline domains back to an isotropic distribution of domain orientations in the absence of an applied field. The stability of such silicate–surfactant mesophase alignments may be useful in allowing subsequent material treatment or analysis outside the orienting magnetic field, with positive implications for materials processing applications.

(34) (a) Luzzati, V. *J. Phys. II Fr.* **1995**, 5, 1649–1669. (b) Clerc, M.; Levelut, A. M.; Sadoc, J. F. *J. Phys. II Fr.* **1991**, 1, 1263–1276. (c) Rançon, Y.; Charvolin, J. *J. Phys. Chem.* **1988**, 92, 6339–6344. (d) Larsson, K.; Fontell, K.; Krog, N. *Chem. Phys. Lipids* **1980**, 27, 321–328. (e) Landry, C. C.; Tolbert, S. H.; Monnier, A.; Norby, P.; Hanson, J. C.; Chmelka, B. F.; Stucky, G. D. Manuscript in preparation.

(35) See, for example: (a) Schnepf, W.; Schmidt, C. *Ber. Bunsenges. Phys. Chem.* **1994**, 98, 248–252. (b) Henriksson, U.; Jonströmer, M.; Olsson, U.; Söderman, O.; Klose, G. *J. Phys. Chem.* **1991**, 95, 3815–3819.

## Conclusions

The liquid crystalline properties of alkaline silicate–surfactant mesophases have been used to create macroscopically aligned systems by exploiting their tendency to orient in high magnetic fields. Alignment on centimeter length scales is achieved by heating the mesophases above their isotropic–anisotropic transition temperature in the absence of silica polymerization, followed by cooling through this transition in an 11.7 T magnetic field. The degree of alignment in lamellar or hexagonal samples can be determined quantitatively with use of deuterated surfactant species by comparison of experimental  $^2\text{H}$  NMR spectra with simulated patterns. Table 1 summarizes the orientational ordering behavior of lamellar and hexagonal liquid crystals formed with different hydrophobic swelling agents. The lamellar and hexagonal mesophase orientations ( $\langle\theta_{\text{DL}}\rangle$ ) with respect to the applied magnetic field depend on the diamagnetic susceptibilities of the constituent molecules, and thus on the composition of a given silicate–surfactant liquid crystal mixture. It is, thus, possible to control the macroscopic orientation of the silicate–surfactant mesophases with respect to the orienting magnetic field by tailoring the composition of the mixture, specifically selecting organic constituents based on their diamagnetic susceptibilities.

These results advance the prospects for obtaining aligned inorganic oxide–surfactant and mesoporous silicate mesophase materials through the use of liquid crystal processing strategies. Although self-assembly and organization can be complicated

by polymerization of the inorganic species (for example silica), and subsequent removal of the surfactant during thermal calcination, preliminary results indicate that aligned structures are preserved after such treatments.<sup>36</sup> Investigations are currently underway in our laboratory to establish protocols for producing orientationally ordered inorganic–surfactant and mesoporous bulk solids, which have promise for new applications in catalysis, separations, and patterned-device development.

**Acknowledgment.** The authors thank Patrick Davidson for helpful discussions. This work was supported by the NSF Young Investigator Program under grant DMR-9257064 (B.F.C.), the David and Lucile Packard Foundation (B.F.C.), Shell Research B.V. (B.F.C.), NSF grant DMR-9520971 (G.D.S.), and NSF grant CHE-9626523 (S.H.T.). The experiments were conducted on NMR instrumentation supported in part by the NSF Division of Materials Research under grant DMR-9222527 and through the UCSB Materials Research Laboratory under award DMR-9632716. A.F. gratefully acknowledges the Henkel Foundation and the American Chemical Society for a Research Fellowship in Colloid and Surface Chemistry. B.F.C. is a Camille and Henry Dreyfus Teacher-Scholar and an Alfred P. Sloan Research Fellow.

JA971267+

---

(36) Tolbert, S. H.; Firouzi, A.; Stucky, G. D.; Chmelka, B. F. Manuscript in preparation.